Population connectivity predicts vulnerability to white-nose syndrome in the Chilean myotis (Myotis chiloensis) - a genomics approach

Thomas M. Lilley *[1], Tiina M. Sävilammi TM †, Gonzalo Ossa ‡§, Anna S Blomberg †, Anti Vasemägi **, Veronica Yung ††, David L.J. Vendrami ‡‡, Joseph S Johnson §§

* Finnish Museum of Natural History, University of Helsinki, Helsinki, Finland.
† Department of Biology, University of Turku, Turku, Finland.
‡ ConserBat EIRL, San Fabian, Chile
§ Programa para la Conservación de los Murciélagos de Chile, Santiago, Chile
** Department of Aquatic Resources, Swedish University of Agricultural Sciences, Uppsala, Sweden
†† Sección Rabia, Subdepartamento de Enfermedades Virales, Instituto de Salud Pública, Santiago, Chile
‡‡ Department of Animal Behavior, University of Bielefeld, Bielefeld, Germany
§§ Department of Biological Sciences, Ohio University, Athens, Ohio

Corresponding author: Thomas M. Lilley

ORCiD:

Thomas M. Lilley 0000-0001-5864-4958

David L.J. Vendrami: 0000-0001-9409-4084

Data availability

The RAD sequencing reads were deposited at NCBI SRA under BioProject ID PRJNA596389.

Running title: Population structure of *Myotis chiloensis*

Key words: Population genetics, population connectivity, population structure, chiroptera, disease spread.

[1] Finnish Museum of Natural History, P. Rautatiekatu 13, University of Helsinki, PL 17, 00014 Helsinki, Finland

Phone: +358408337783

Email: thomas.lilley@helsinki.fi

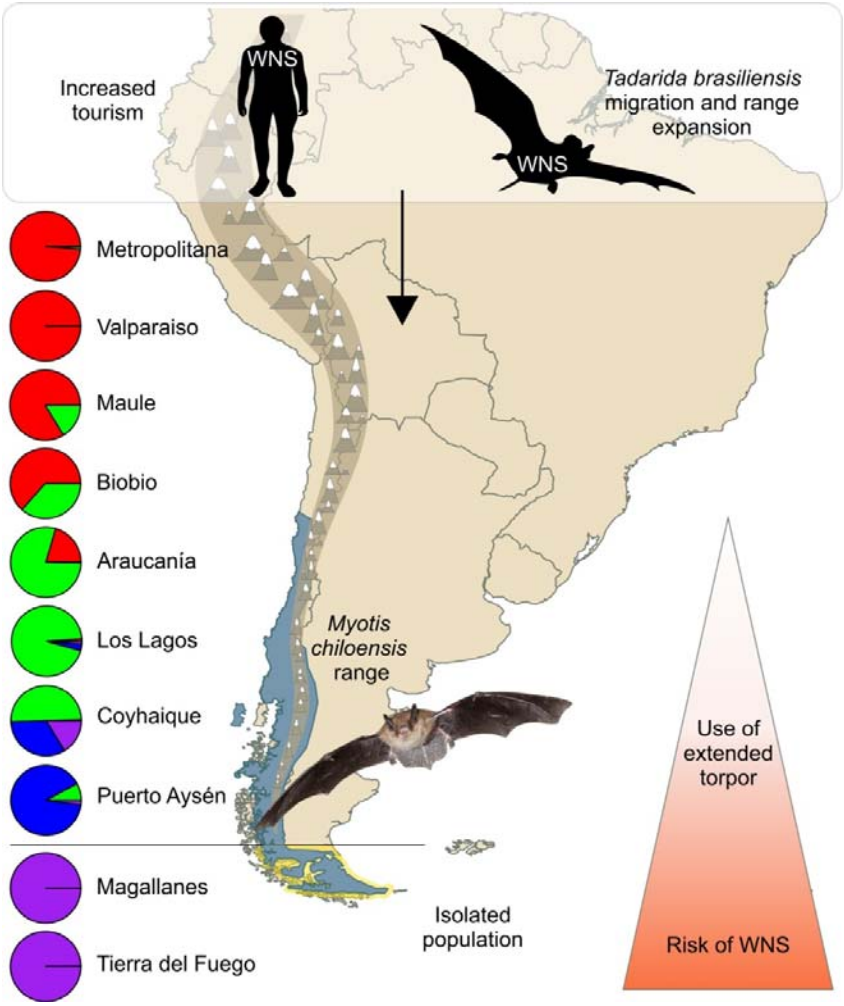

Graphic abstract: Hibernatory populations of *M. chiloensis* are at risk of suffering from bat white-nose syndrome, because of increased tourism and the increase in the range of a possible vector for the disease, *Tadarida brasiliensis*. However, the southernmost hibernatory population, appears to be isolated from more northerly populations, decreasing the risk of spread through contact and mixing with conspecifics from other populations.

ABSTRACT

Despite its peculiar distribution, the biology of the southernmost bat species in the world, the Chilean myotis (*Myotis chiloensis*), has garnered little attention so far. The species has a north-south distribution of c. 2800 km, mostly on the eastern side of the Andes mountain range. Use of extended torpor occurs in the southernmost portion of the range, putting the species at risk of bat white-nose syndrome (WNS), a fungal disease responsible for massive population declines in North American bats. Here, we examined how geographic distance and topology would be reflected in the population structure of *M. chiloensis* along the majority of its range using a double digestion RAD-tag method. We sampled 66 individuals across the species range and discovered pronounced isolation-by-distance. Furthermore, and surprisingly, we found higher degrees of heterozygosity in the southernmost populations compared to the north. A coalescence analysis revealed that our populations may still not have reached secondary contact agter the Last Glacial Maximum. As for the potential spread of pathogens, such as the fungus causing WNS, connectivity among populations was noticeably low, especially between the southern hibernatory populations in the Magallanes and Tierra del Fuego, and more northerly populations. This suggests the probability of geographic spread of the disease from the north through bat-to-bat contact to susceptible populations is low. The study presents a rare case of defined population structure in a bat species and warrants further research on the underlying factors contributing to this.

Key words: population structure, Myotis, Chiroptera, opportunistic pathogen, disease spread

71 INTRODUCTION

72 Transmission of infectious diseases has garnered attention as one of the greatest risks to
73 human, agriculture and wildlife health over the last decade (Cangelosi *et al.* 2004; Semenza
74 and Menne 2009). Previous research demonstrates that the emergence of previously
75 unknown diseases often results from a change in the ecology of the host, pathogen, and/or
76 their environment (Scholthof 2007). An example of this is white-nose syndrome (hereafter
77 WNS), an epizootic disease that emerged in North America in 2006 (Blehert *et al.* 2009). The
78 disease is caused by the fungus, *Pseudogymnoascus destructans*, which infects insectivorous
79 bats during the hibernation period at latitudes where prey are not widely available during
80 winter (Lorch *et al.* 2011). Populations of highly susceptible species, especially from the
81 genus *Myotis*, have declined by >90% in areas affected by WNS (Frick *et al.* 2010). The
82 opportunistic pathogen can utilize alternative carbon sources (Raudabaugh and Miller 2013)
83 and can persist in the cold, humid environment within hibernacula in the absence of bat
84 hosts (Lorch *et al.* 2013; Hoyt *et al.* 2014).

85 *P. destructans* is native to Eurasia, where it has a large geographic range, with transmission
86 to North America likely facilitated by humans (Warnecke *et al.* 2012; Leopardi *et al.* 2015).
87 In North America, bats suffering from WNS were first detected in the state of New York
88 during the winter of 2006–2007 (Frick *et al.* 2010). The fungus has since spread across North
89 America, with records of prevalence in 33 U.S. states and 7 Canadian provinces. So far, *P.*
90 *destructans* has been detected on 17 species of bats, with more species likely to follow.
91 While human-assisted transmission of *P. destructans* likely has contributed to this spread,
92 the ecology and behaviour of cave-hibernating bats in North America also makes them
93 efficient vectors over large geographic areas (Wilder *et al.* 2015). Because WNS affects bats
94 during extended bouts of torpor, at low temperatures where it is able to grow and infect the
95 host, there has been speculation over how far into the southern North America the disease
96 will spread (Verant *et al.* 2012; Meierhofer *et al.* 2019). Although bats inhabiting lower
97 latitudes may suffer less from WNS, *P. destructans* conidia may be able to survive on the
98 body of bats for several months, even at temperatures up to 37 °C (Campbell *et al.* 2019).
99 This could facilitate the movement of WNS across Mesoamerica and the tropics, to arrive to

high southern latitudes where bats may be susceptible (Holz *et al.* 2019; Turbill and Welbergen 2019).

Of species known to harbour the WNS fungus, *Tadarida brasiliensis* is of particular interest. As a long-range migratory species, with movements spanning thousands of kilometres (Cockrum 1969; Glass 1982), *T. brasiliensis* may be an important vector for spreading *P. destructans* into the southern hemisphere (Ommundsen *et al.* 2017; McCracken *et al.* 2018). Ecological niche models predict suitable habitat for the proliferation of *P. destructans* in South America, highlighting the need to understand vectors such as *T. brasiliensis* as well as human transmission (Escobar *et al.* 2014). However, once *P. destructans* arrives in South America, its spread will not necessarily resemble that seen in North America, as it is likely to be influenced by differing geology and species ecology.

The Chilean myotis (*Myotis chiloensis* [Waterhouse, 1840]) is the most Southerly distributed species of bat in the world, together with the southern big-eared brown bat (*Histiotus magellanicus*, Koopman 1967; Gardner 2007). *Myotis chiloensis* has a vast north-south distribution that includes forested areas on both sides of the Andes from the northern shore of Navarino Island to the southern border of the Atacama desert in Chile (Ossa and Rodriguez-San Pedro 2015). Most of the distribution range of *M. chiloensis*, overlaps with the distribution of *T. brasiliensis*, from the north, where *M. chiloensis* is not believed to hibernate, to 45°S of latitude, where *M. chiloensis* possibly hibernate and may therefore be susceptible to WNS (Bozinovic *et al.* 1985). However, there is no information available on the population structure of *M. chiloensis*, precluding an understanding of how *P. destructans* could be transported from the northern edge of its range to more southern, and vulnerable, populations. The connectedness of individuals across the range of the species will determine the speed and intensity of potential spread. Population structuring in bats is often relatively low because of their efficient mode of dispersal, flight (Laine *et al.* 2013). An ability to disperse more efficiently results in decreased population differentiation (Bohonak 1999) to the extent that some bat species are panmictic across their range (Burland and Wilmer 2001; Laine *et al.* 2013). Such high dispersal would likely result in rapid spread of *P. destructans*. However, bats in the genus *Myotis* show instances of pronounced population structure that may hinder spread of the fungus. For instance, the Gibraltar Strait, which

130 separates the Iberian Peninsula from the Maghreb in Morocco by a minimum gap of 14 km
131 of the open sea, represents a barrier for gene flow for *M. myotis* (Castella *et al.* 2000). Chile
132 is littered with such potential barriers to gene flow, such as the Atacama Desert, glaciers, ice
133 fields, the Andes Mountains, and the Magellan Strait, which in turn can hinder the potential
134 spread of *P. destructans*. Furthermore, populations may still be affected by the Last Glacial
135 Maximum, which covered a large part of Patagonia under ice until c. 10000 years bp (Sérsic
136 *et al.* 2011; Mansilla *et al.* 2018).

137 With tourism in southern Chile expected to increase (e.g. . http://www.conaf.cl/parques-
138 nacionales/visitanos/estadisticas-de-visitacion/), and migratory species such as *T.*
139 *brasiliensis* capable of carrying spores across large distances, there is a serious need to
140 better understand the population structure of Patagonian hibernatory bat species before
141 WNS spreads to the region. The lack of knowledge on the extent of migration and mixing,
142 and life history traits in general, means that research in this area is now urgent and essential
143 (Ossa and Rodriguez-San Pedro 2015; Ossa 2016; Ossa *et al.* 2019). Studying population
144 ecology through molecular genetic methods allows for the identification of more accurate
145 population boundaries, which is important when assessing conservation in response to
146 threats of disease and dramatic declines in population size (Moritz 1994). This study will
147 therefore aim to describe population structure and isolation-by-distance in *M. chiloensis*
148 across the range of the species. By studying *M. chiloensis* along 2400 km of latitudinal
149 gradient using genome-wide SNP markers, we aimed to test if geography and the Last
150 Glacial Maximum influence genetic isolation patterns.

151 MATERIALS AND METHODS

152 Sample collection and DNA extraction

153 To describe population genetic structure in *M. chiloensis*, we obtained wing tissue samples
154 of 66 bats from two sources. A portion were obtained from live bats captured in the field
155 during November and December 2017 (i.e. austral spring) from two localities: Chicauma,
156 Metropolitana region (33 °S 70 °W) and Karukinka Reserve, Tierra del Fuego (64 °S 78 °W)
157 respectively (Capture permit: 4924_2017, Figure 1 A, Table S1). We used disposable biopsy
158 punches (5 mmm, MLT3335, Miltex Instrument Co, Plainsboro, New Jersey) to collect

159 samples from captured bats, which were then released at the capture site. Additional
160 samples were obtained from dead bats submitted to the Public Health Institute of Chile for
161 rabies testing (Figure 1 A, Table S1). Submitted bats included latitude and longitude
162 locations of their origin. Tissue samples from these bats were obtained from the
163 plagiopatium using sterile scalpels. To determine if *P. destructans* had already spread to
164 Chile, we swabbed the nose and wings of all bats in the field and at the Public Health
165 Institute of Chile bat with a sterile polyester swab (Puritan 25-806 1PD, Guildford ME, USA)
166 and stored at -20 °C until analysis.

167 We divided samples into four groups according to their geographic origin, with sub-locations
168 within each group to assist in further analyses. Sampling locations are presented in Figure 1
169 A and details of populations and samples are provided in Table 1 and Table S1. Tissue
170 samples were stored in 1.5 ml tubes with 95% EtOH and stored at -20 °C until further
171 analysis. Fungal spore samples were stored in 1.5 ml tubes and stored at -20 °C until further
172 analysis. We extracted DNA from tissue samples using QIAmp DNA Mini Kits (Qiagen, Hilden
173 Germany) and stored DNA at -80 °C. DNA from fungal swabs was extracted using Qlamp
174 DNA Micro Kits (Qiagen, Hilden Germany).

175 The amount of DNA in the final solution of each sample was tested and quantified using the
176 Thermo Scientific Nanodrop spectrophotometer, giving a result for the amount of DNA in
177 ng/ µL. Samples were frozen between DNA extraction and analysis.

178 Identification and quantification of *P. destructans*

179 Quantification of *P.destructans* load by qPCR was completed as described previously in
180 Johnson et al. (2015) with the exception of using 1 µl sample in the reaction, Roche Fast
181 Start Essential DNA Probe Master, and a Roche Lightcycler 480 instead of a BioRad iCycler.

182 RAD sequencing

183 We sampled 66 bats, including duplicate tissue samples from 30 individuals to estimate
184 repeatability and error rate of the called genotypes. DNA was prepared for genotyping-by-
185 sequencing using a double digestion RAD-tag method as described in Elshire et al. (2011).
186 PstI-BamHI-digested libraries were prepared by the Center of Evolutionary Applications

187 (University of Turku; see Lemopoulos et al. 2017 and references therein for further details)
188 and sequenced in an Illumina HiSeq2500 run (100 bp single end reads and pooling 96
189 samples on each lane) at Finnish Functional Genomics Centre (Turku Bioscience).

190 Yield comparison samples

191 As the amount of DNA available may often be very limited in experiments where preserved
192 samples from the rabies laboratory are utilized, we wanted to estimate the effect of initial
193 DNA concentration to the resulting read coverage. We compared the total read coverages
194 of the replicate samples with Pearson's correlation.

195 The resulting fastq reads, separated by barcode for each sample, were quality-controlled
196 and low-quality bases trimmed with condetri v. 2.3 with parameter minlen=30 (min. length
197 of a trimmed read) followed by adapter-trim with cutadapt for Illumina universal adapters
198 from the end of the reads (identified with FastQC quality control in some of the samples).
199 Then, reads were mapped against *M. lucifugus* genome (mluc_2.0_assembly_supers.fasta)
200 using bwa mem with parameters -B 3 -O 5 -k 15. After mapping back with BWA mem, we
201 used SAMtools v. 1.4 and the associated bcftools for calling genotypes for SNPs and for
202 filtering SNPs based on minimum of 40% of the samples genotyped, at least eight
203 alternative alleles detected and SNP quality >=20 (bcftools filter). We further filtered the
204 SNPs based on exactly two alleles detected and excluded SNPs with particularly low (≤5) or
205 unusually high (≥125) mean coverage based on visual inspection of the mean coverage
206 distribution.

207 Population genetic analysis

208 For the final SNP dataset, which only included unduplicated samples, we performed
209 principal component analysis implemented in prcomp function of R stats package, and
210 calculated Euclidean genetic coordinates for each individual from PC1 and PC2. The four
211 pre-determined ancestral populations based on the sampling regions of each individual
212 were confirmed by hierarchical clustering of the Euclidean distanced calculated from PC1
213 and PC2. Individuals clustering to a neighbouring population were assumed to have
214 dispersed from their natal populations and were reassigned for the later analysis. We
215 further investigated the relative contributions of the ancestral populations inhabiting

regions 1-4 in the present-day nucleotide using ADMIXTURE (Zhou et al. 2009) analysis for the A-samples, run with four expected populations (parameter K=4) based on prior knowledge of the population structure, and with quasi-Newton convergence acceleration method. We were particularly interested in identifying possible hybrid individuals.

After assigning each individual to the final regions, we calculated Nei's pairwise F_{ST} using HierFSTat v. 0.04-22 pairwise. FST function for A-samples for SNP's with no missing values. To assess the significance of genetic differentiation, we compared the actual obtained F_{ST} estimates to the null distributions of F_{ST} values under panmixia, obtained from a hundred random permutations of alleles. Latitude and longitude coordinates of the sampling locations were used to calculate pairwise geographic distances between individuals in kilometres using Haversine method assuming a spherical earth, implemented in function distm in the R package geodist v. 1.5-10.

We estimated Isolation-by-distance with two methods: A Mantel test with complete permutations and a linear model *geographic distance ~ genetic distance*. We used pairwise F_{ST} as a measure for the genetic distances and mean of between-individual distances as geographic coordinates for populations inhabiting each of the four regions. To study the population structure in more detail, we repeated the Isolation-by-distance analysis for the genetic vs. geographic distances from the most extreme individual (sample ID 700) using a Mantel test with all possible permutations, and a linear model to identify individuals with unusually high or low genetic differentiation. We then studied the systematic differentiation of the individuals sampled in different regions by assessing the differences of the residual distributions of each of the four populations from zero using t-tests and Bonferroni-correction of the *P*-values.

We also calculated mean observed heterozygosity within the variable loci in Hardy-Weinberg equilibrium (*FDR*>=0.05) in each of the four study regions and compared the observed values to the mean expected heterozygosities using inbreeding coefficient *F,* calculated as the difference between expected and observed heterozygosity divided by expected heterozygosity (Serre 2006). The 95% confidence intervals for the heterozygosity estimates were found by randomly sampling the variable loci for 1,000 times and extracting the distributions of bootstrap means. The deviations of *F* statistics from zero were detected

246 using single-sample Wilcoxon tests. The significances of the regional differences in the
247 observed and expected heterozygosity distributions, and in the F statistics, were tested both
248 by inspecting the overlaps in the bootstrapped confidence intervals and using analysis of
249 variance and Tukey's post hoc tests. The significances of within-region differences between
250 the expected and observed heterozygosity were tested both by comparing the
251 bootstrapped confidence intervals and by pairwise t-tests and Bonferroni-corrected p-
252 values. Finally, the fraction of SNPs unique to any one region, and the number of SNPs
253 shared between all regions, were calculated from the observations of variable and non-
254 variable loci within regions.

255 Demographic modeling

256 To formally test whether any of the studied populations experienced secondary contact
257 following glaciation, we implemented a demographic analysis using the software
258 *fastsimcoal2* (Excoffier *et al.* 2013) in combination with the folded site frequency spectra
259 (SFS) calculated from our data using easySFS.py utility (available from
260 https://github.com/isaacovercast/easySFS). Specifically, we evaluated support for two
261 alternative models (Supplementary Figure S6). The first model, representing our null
262 hypothesis of no secondary contact among populations, specified four distinct lineages
263 (region 1, region 2, region 3 and region 4) corresponding to the populations inhabiting the
264 four geographic regions sampled in the present study. These diverged from each other at
265 the time points T1, T2 and T3 as presented in Figure S6a, and exchanged no migrants.
266 Region 1 was used as the lineage from which the other three populations emerged, as this is
267 thought to be the population which is closest to the ancestral *Myotis chiloensis* population.
268 The second model, representing our alternative hypothesis of secondary contact among
269 populations, was identical with the exception that symmetric migration was present
270 between population pairs region 1- region 2 and region 3- region 4, and asymmetric
271 migration was implemented from region 2 to region 3 (Supplementary Figure S6b). In
272 addition to identify the model that was best supported by our data, we also estimated
273 divergence times (T1, T2 and T3) and effective population sizes (region 1, region 2, region 3
274 and region 4) for the four modeled lineages, as well as migration rates (Mig12, Mig21,
275 Mig34, Mig43 and Mig32).

276 We performed 50 independent *fastsimcoal2* runs for each model, with 100,000 simulations
277 and 40 cycles of the likelihood maximization algorithm. We then calculated Akaike's
278 Information Criteria (AIC) from the *fastsimcoal2* runs which yielded the highest maximum
279 likelihood for each model and used these values for model comparison. Finally, we
280 extracted parameter estimates from the best run of the most supported model and
281 calculated 95% confidence intervals based on 100 parametric bootstrap replicates, as
282 described in Excoffier et al. (2013).

283 Data availability

284 The RAD sequencing reads were deposited at NCBI SRA under BioProject ID PRJNA596389.

285 RESULTS

286 Filtering

287 Ninety-one of the 96 samples (66 individuals and 30 duplicates) had reads matched with a
288 barcode. Of the obtained genotypes, 54846 were biallelic and used in the later analysis,
289 while we excluded 88882 non-variable (homozygous to alternative) variants and 1708
290 variants with more than 2 alleles. After filtering, the mean SNP coverage ranged from 0.5 to
291 257.0 (Supplementary Figure S1). We excluded tags with <5 or > 125 mean coverage, leaving
292 47079 tags. The average rate of missing SNPs among the final unique samples was 6.2%,
293 ranging from 0 to 24%.

294 Replicate samples

295 The correlation between input DNA concentration and the resulting mean per-sample read
296 coverage was only moderate (cor = 0.3394, t_{61} = 2.8178, P = 0.0065, Supplementary Figure
297 S2 A, Supplementary Figure 3 A-B). In contrast, we found strong and negative association
298 between mean read coverage after sequence assembly and the number of missing genotype
299 calls (cor = -0.9763, t_{61} = -35.223, P < 2.2e-16, Figure S2 B). Furthermore, read coverages
300 were very similar between the technical replicate samples (cor = 0.8736, t_{26} = 9.1542, P =
301 1.292e-09, Supplementary figure S2 C), allowing us to omit "B" samples (replicated). The
302 removal of the biological replicates was conducted to minimise the possible SNP calling bias
303 induced by some samples having approximately twice the amount of sequence data

304 compared to the others, if replicate samples had been combined. Identical genotype calls
305 ranged from 85.6% to 96.9% with an average of 94.2% identical genotype calls
306 (Supplementary figure S3 C), depending heavily on read coverage (cor = 0.9275, t_{26} = 12.641,
307 *P* = 1.312e-12 and cor = 0.8484, t_{26} = 8.1716, *P* = 1.186e-08 in "A" and "B" samples,
308 respectively; Supplementary figure 2 E-F). Although the correlation between the initial DNA
309 concentration and identical genotype calls between biological replicates was significant (cor
310 = 0.5990, t_{26} = 3.814, *P* = 0.0007579; Supplementary figure S2 D), this seemed to mainly be
311 due to two outlier observations with both very low concentration and repeatability.

312 Identification and quantification of *P. destructans*

313 Besides our control samples, no samples showed signs of amplification a portion of the
314 multicopy intergenic spacer region of the rRNA gene complex of *P. destructans* by 38 cycles,
315 which is generally considered as a cut-off for the presence of the pathogen DNA in the
316 samples (Muller *et al.* 2013). Therefore, we can conclude that the *M. chiloensis* individuals
317 sampled in this study did not carry *P. destructans*.

318 Population genetic analysis

319 Principal component analysis on 66 individuals and 5538 SNPs without any missing values
320 from non-duplicated samples (label including A, Figure 1 B) revealed a clear structuring of
321 individuals according to the sampling location indicative of strong population structure.
322 Based on hierarchical clustering of the two most important principal components
323 (Supplementary Figure 4), we confirmed the four pre-determined populations based on the
324 natural hierarchical structuring of the data. Based on the clustering, the sub-population
325 assignment of one individual, sample number 679, changed from Biobio to Maule (which
326 was the most common region assignment among the three nearest neighbors for that
327 individual). The estimation of ancestry of each sampled individual by examining the relative
328 contributions of ancestral populations inhabiting regions 1-4 in the present-day revealed
329 particularly pure ancestral lines in the northern and southern parts of the range, with
330 hybridization occurring in the central part of the range (Figure 2.).

331 Pairwise F_{ST}-value estimates between the populations sampled from the four geographical
332 locations ranged from 0.04 (between regions 2 and 3) to 0.113 (between the most distant

333 regions 1 and 4, Table 2). All estimated F_{ST} values were found significantly larger (P<0.01)
334 than the permuted F_{ST} distributions, with the 95 % confidence intervals of the null
335 distributions between 0 and 0.0205. Both the Mantel test approach and linear modelling
336 between genetic distances (Euclidean distances calculated from PC1 and PC2) and
337 geographical distances (latitude/longitude coordinates converted to distances in kilometres)
338 strongly suggested that we reject the null hypothesis of geographic and genetic distances
339 being unrelated. For the between-population comparisons with F_{ST}, we calculated Mantel
340 statistic r = 0.9497 (P = 0.041667) and R-squared estimate of 0.8773 (DF = 1,4, t = 6.063, P =
341 0.00374) (Supplementary figure 5. Also, for the between-individual distances, the observed
342 Mantel statistic r = 0.944 (P = 0.001), and R-squared estimate 0.943 (DF = 1,61; t = 31.994; P
343 < 2e-16) from the linear modelling suggesting that genetic and geographic distances are
344 strongly positively associated (Figure 3). More detailed exploration of the between-
345 individual linear model revealed, that the distribution of the residuals in regions 1 (DF = 20, t
346 = -3.0679, Bonferroni P = 0.024284) and 4 (DF = 11, t = -10.523, Bonferroni P = 1.7724e-06)
347 were marginally smaller than 0, while the residuals of individuals in regions 2 (DF = 15; t =
348 3.5896; adj. Bonferroni P = 0.002682) and 3 (DF = 13, t = 5.9325, Bonferroni P = 0.0001986)
349 were significantly larger than 0 (Figure 3).

350 Of the total of 47079 SNPs, 43903 were found to be in Hardy-Weinberg equilibrium.
351 Analyses of variance revealed statistically significant differences between populations in
352 observed heterozygosities [F(3,106450)=760.6, P<2e-16], in expected heterozygosities
353 [F(3,106450)=871.4, P<2e-16], and in the F statistics [F(3,106450)=55.29, P<2e-16]. Both
354 based on confidence intervals and pairwise comparisons, observed and expected
355 heterozygosity distributions were consistently higher (non-overlapping 95% confidence
356 intervals and adjusted P<0.05) in the southern regions than in north, except for the two
357 northernmost regions (region 1 vs. region 2), where a statistically significant difference was
358 not observed (Table 1, Table S2). Similarly, observed heterozygosities were consistently
359 lower than those estimated from allele frequencies (non-overlapping 95% confidence
360 intervals and adjusted P<0.05), which may be caused by within-region population structure
361 (Table 1, Table S2). Finally, pairwise comparisons of the inbreeding coefficient distributions
362 indicated that the excess of homozygotes was greater in the north than in the south when
363 compared to neutral expectation based on allele frequencies. This was supported with

364 statistically significant differences (non-overlapping confidence intervals and adjusted
365 $P<0.05$) observed in all comparisons except in region pairs 2 and 3; and 4 and 5 (Table 1,
366 Table S2). This indicated that the northern populations are inbreeding more than the
367 southern populations (Table 1, Table S2).

368 A large proportion of SNPs, 25.3%, were polymorphic in all four regions. The fraction of
369 SNPs unique only to one region decreased from going north to south: while 8.6% of the
370 SNPs were unique to region 1, only 2.5% unique SNPs were found in region 4.

371 We did not find support for secondary contact using demographic modelling with
372 Fastsimcoal2. Instead, the null model that included no migration among populations (Figure
373 S6a) received the highest AIC support (Table S3). Parameter priors and estimates, together
374 with their 95% confidence intervals, from the best model are reported in Table S4.

375 DISCUSSION

376 Our results present the first assessment of population structure in the widely distributed bat
377 species, *M. chiloensis*, using individual-based approach with genome-wide markers. We
378 found that geographic distance within the range of the species are reflected in its
379 population structure. Although we found a clear and robust population structure among
380 sampling sites, population structure is correlated with geographical distance, even though
381 populations are separated by ice fields, mountain ranges and stretches of open water. This
382 has implications for the protection of populations that may be susceptible to WNS. Our
383 results also show highest genetic variability in the species is at the southern extent of its
384 range.

385 Strong population structure is rarely seen in bats, even across large geographical scales in
386 genera such as *Myotis*, with shorter dispersal distances (Castella *et al.* 2000; Atterby *et al.*
387 2010; Laine *et al.* 2013). In fact, geographical distance often correlates significantly with
388 genetic distance in bats. This is partially due to autumn migration and swarming behaviour
389 in *Myotis* species, which brings together bats from broad geographic areas to breed and
390 promote recombination (Burns *et al.* 2014; Burns and Broders 2015). Furthermore, powered
391 flight allows effective dispersal, which is often male biased (Arnold 2007; Angell *et al.* 2013).
392 This is reflected in low fixation indices in widespread bat species, such as *M. daubentonii*,

393 where individuals separated by thousands of kilometres in Europe show low fixation indexes
394 (Laine *et al.* 2013). While fixation indices cannot be compared directly across species,
395 especially when different methodological approaches are used, they do give an indication of
396 the connectivity of populations.

397 Although geographic and genetic distances were found to have a strong positive correlation
398 in our study, we can concur that the southernmost population shows a higher degree of
399 isolation compared to the geographic distance to its closest comparative population to the
400 north. An F_{ST} of 0.075 between regions 3 and 4 using whole-genome data is already higher
401 than F_{ST} values recorded for *M. daubentonii* across Europe using microsatellites (Laine *et al.*
402 2013), and in our data, the geographic distance is only c. 1000 km. Our data, with tens of
403 thousands of SNP's also allowed a more precise estimate of fixation compared to a handful
404 of microsatellites. However, due to a limited number of individuals, it did not allow us to
405 examine dispersal as a function of sex, which in bats is often a male driven function (Arnold
406 2007; Laine *et al.* 2013; Angell *et al.* 2013). Our sampling may also have missed some
407 connecting populations in between regions 3 and 4, which could for instance be located on
408 the eastern slopes of the Andes. However, our test for relative contributions of ancestral
409 populations reveals bats in region 4, in the Magallanes and Tierra del Fuego, have no mixing
410 of ancestral populations with the other regions.

411 In the northern hemisphere, approximately 18000 years ago, at the end of the Late
412 Pleistocene, the ice sheets began to recede as the global climate became warmer. The biota
413 migrated northwards following their optimal environments (Huntley and Webb 1989). This
414 expansion of refugial populations has been associated with genetic variation decreasing
415 south-to-north in some species: a trend attributed to a series of bottlenecks when the biota
416 spread from the leading edge of the refugial population, leading to a loss of alleles and
417 decreasing genetic diversity (Hewitt 1996, 1999). Contrary to what one could expect based
418 on these latitudinal shifts in diversity in the northern latitude, genetic diversity in *M.*
419 *chiloensis* appears to increase with increasing latitude, from north to south. We presumed
420 this counterintuitive pattern of heterozygosity within the species may be related to the
421 glaciation history of South America, where populations isolated by glacial events could have
422 been able to hybridize. For instance, in some terrestrial European and Scandinavian

423 vertebrates, the intraspecific genealogical lineages, which formed in separate refugia, were
424 found to have come to secondary contact in the Fennoscandian area (Tegelström 1987;
425 Jaarola and Tegelström 1995; Nesbø *et al.* 1999; Knopp and Merilä 2009).

426 *Myotis chiloensis* is described as a vicariant species with respect to other closely related
427 *Myotis* species (*M. albescens, M. nigricans, M. levis*) from South America, Ruedi et al (2013)
428 estimated this isolation event at 5.5 My in late Miocene. This same time period saw the
429 beginning of a number of glaciations events in Patagonia with variable intensity and
430 duration (Rabassa *et al.* 2011). Glacial episodes isolated the Patagonian forest from around
431 middle Miocene well into the late Quaternary, the Last Glacial Maximum (Rabassa *et al.*
432 2011, Supplemental Figure S7). During the glaciations, the forests on the Pacific coast were
433 most like completely suppressed, possibly with isolated small refugia. On the Atlantic side,
434 the forest was fragmented from 36°S southwards (Sérsic *et al.* 2011). Finally, in Tierra del
435 Fuego the forest was probably displaced towards the current submarine shelf (Ponce *et al.*
436 2011). As the ice retreated refugial populations may have come into secondary contact in
437 the southern part of current range, which could explain the high heterozygosity as well as
438 the small fraction of unique SNP's of these populations. However, our coalescence analysis
439 rejected the secondary contact model, favouring the null model suggesting our study
440 populations are still largely separated after the Last Glacial Maximum. Indeed, the F_{ST} -
441 values are high, suggesting isolation of the populations. By contrast, our analysis for the
442 relative contributions of ancestral populations suggests mixing of populations. One potential
443 explanation for this apparent discrepancy is that we derived Site Frequency Spectrum from
444 a rather small number of individuals, which may carry a signal of migration that is not strong
445 enough to allow a model that includes secondary contact to be favoured over a simpler
446 model without migration.

447 The spread of *P. destructans* via one host to another was very rapid in North America
448 (Blehert *et al.* 2009; Frick *et al.* 2010). This was facilitated in part by the ecology of North
449 American cave-hibernating bats and the availability of suitable environment for the fungus
450 to propagate: limestone caves found throughout the Appalachian region in eastern North
451 America (Lorch *et al.* 2013). Furthermore, as a consequence of down-regulation of
452 metabolism during extended torpor bouts, attempted immune responses fall short, and

453 may even contribute to mortality in hosts infected with *P. destructans* (Field *et al.* 2015;
454 Lilley *et al.* 2017, 2019). In addition to these, the massive population declines associated
455 with WNS in affected species (Turner *et al.* 2011) were magnified by the panmictic
456 population structure across eastern North America in the most affected species, *M.*
457 *lucifugus* (Miller-Butterworth *et al.* 2014; Vonhof *et al.* 2015).

458 Our results for *M. chiloensis* from austral South America suggest the southernmost
459 population in region 4, may be less likely to be infected via their continental conspecifics,
460 because of reduced contact between the populations. Our results indicated no mixing of
461 ancestry in the southernmost individuals in our study, suggesting the *M. chiloensis* on Tierra
462 del Fuego are isolated from their mainland counterparts. To our knowledge, this is also the
463 only population to use extended torpor, a prerequisite for the propagation of *P. destructans*
464 and the onset of WNS (Ossa *et al.* Submitted for publication). Tierra del Fuego, the southern
465 tip of Patagonia and the continent of South America, experiences extended low winter
466 temperatures comparable to areas in North America where WNS is manifested. Our genetic
467 analysis for the presence of *P. destructans* on the sampled bats suggests the fungal
468 pathogen does not exist within the distribution range of our focal species at present. Even if
469 the fungus were to enter the region, variability in host behavior and environmental
470 characteristics may be the primary factors protecting hosts from the pathology related to
471 WNS (Zukal *et al.* 2014, 2016). Most strikingly large cave hibernacula with suitable, stable
472 environmental conditions favouring the environmental persistence of the pathogen in the
473 absence of the hosts, are very scarce and separated by hundreds of kilometers in most of
474 the southern range of *M. chiloensis*.

475 The observed distribution of *M. chiloensis* is vast, covering a range of forested habitats from
476 arid Sclerophyllous to sub-Antartic (Ossa and Rodriguez-San Pedro 2015). In this respect,
477 taking into consideration our results on clear population segregation begs to propose the
478 question on the species status of *M. chiloensis* as a whole. Indeed, *M. chiloensis* also
479 appears to vary phenotypically along its distribution range (Mann 1978; Ossa 2016). It has
480 been proposed that the species was composed of three sub-species: *M. ch. atacamensis*
481 which is presently known as *M. atacamensis; M. ch. arescens* from 29°S to 39°S; and *M. ch.*
482 *chiloensis* from 39°S to 53°S (Mann 1978). That classification was due according to their coat

483 colour changes in relation to exposure to solar radiation and ambient temperature, which is
484 correlated to latitude (Budyko 1969) and levels of precipitation in their habitat. They vary
485 from a lighter pelage to a dark brown colour on a gradient from the northern part of their
486 range to the south (Galaz *et al.* 2006). This promotes the theory, isolation by adaptation, as
487 a driver of population genetic structure. The genetic adaptations of an individual to their
488 local environment separates populations and leads to a reduced gene flow (Orsini *et al.*
489 2013). However, the isolation by adaptation theory negates the fact that there is a
490 possibility of a barrier so that gene flow is inhibited by climate or adaptations to the local
491 environment. It is possible to therefore state that isolation-by-dispersal limitation, and
492 moreover isolation-by- distance, are the more probable causes of the observed results in
493 the present study. Indeed, the reluctance of the species to cross barriers, for instance the
494 Andes, can clearly be seen by examining population 3, where six individuals sampled from
495 Puerto Aysén (437, 442, 443, 167, 256, 260) are visibly isolated on the PCA plot form
496 individuals on the other side of the Andes, under 150 km away. This also depicts the fine
497 scale resolution our individual-based SNP-based approach allows. However, further studies
498 should focus deeper on the taxon status of different population of the species currently
499 recognized as *M. chiloensis*.

500 The results highlight the importance to assess the population structure which may limit the
501 spread of white-nose syndrome disease. Whether *P. destructans* or another epizootic in the
502 future could spread depends largely on the population structure and connectedness of
503 hosts (Lilley *et al.* 2018).

504 ACKNOWLEDGEMENTS

505 We thank the Rufford Foundation ((Rufford Small Grant (10502-1 and 23042-2), H2020
506 Marie Skłodowska-Curie Actions (706196), and Ohio University Research Council for funding
507 the work. We thank Servicio Agricola y ganadero Diproren for the capture permits in Tierra
508 del Fuego (Res Ex: 1253/2016 and 4924/2017) , Juan Carlos Aravena from the Instituto de la
509 Patagonia for his help, the personnel from WCS Chile for allowing us to conduct research at
510 Karukinka Natural Reserve as well as for their help with field work. We thank Michelle
511 Lineros and Tania Gatica from the National Health Institute for their help to obtain the
512 tissue samples. We thank Austin Waag for assistance with field work.

513 REFERENCES

514 Angell, R. L., R. K. Butlin, and J. D. Altringham, 2013 Sexual segregation and flexible mating
515 patterns in temperate bats. Plos One 8:.

516 Arnold, B. D., 2007 Population structure and sex-biased dispersal in the forest dwelling
517 vespertilionid bat, *Myotis septentrionalis*. Am. Midl. Nat. 157: 374–384.

518 Atterby, H., J. Aegerter, G. Smith, C. Conyers, T. Allnutt *et al.*, 2010 Population genetic
519 structure of the Daubenton's bat (*Myotis daubentonii*) in western Europe and the
520 associated occurrence of rabies. Eur. J. Wildl. Res. 56: 67–81.

521 Blehert, D. S., A. C. Hicks, M. Behr, C. U. Meteyer, B. M. Berlowski-Zier *et al.*, 2009 Bat white-
522 nose syndrome: an emerging fungal pathogen? Science 323: 227–227.

523 Bohonak, A. J., 1999 Dispersal, gene flow, and population structure. Q. Rev. Biol. 74: 21–45.

524 Bozinovic, F., L. Contreras, M. Rosenmann, and J. Torres-Mura, 1985 Bioenergetics of *Myotis*
525 *chiloensis* (Quiroptera: Vespertilionidae). Rev Chil Hist Nat 58: 39–45.

526 Budyko, M. I., 1969 The effect of solar radiation variations on the climate of the Earth. Tellus
527 21: 611–619.

528 Burland, T. M., and J. W. Wilmer, 2001 Seeing in the dark: molecular approaches to the
529 study of bat populations. Biol. Rev. 76: 389–409.

530 Burns, L. E., and H. G. Broders, 2015 Who swarms with whom? Group dynamics of *Myotis*
531 bats during autumn swarming. Behav. Ecol. 26: 866–876.

532 Burns, L. E., T. R. Frasier, and H. G. Broders, 2014 Genetic connectivity among swarming
533 sites in the wide ranging and recently declining little brown bat (*Myotis lucifugus*).
534 Ecol. Evol. 4: 4130–4149.

535 Campbell, L. J., D. P. Walsh, D. S. Blehert, and J. M. Lorch, 2019 Long-term survival of
536 *Pseudogymnoascus destructans* at elevated temperatures. J. Wildl. Dis.

537 Cangelosi, G., N. Freitag, and M. Riley-Buckley, 2004 From outside to inside: environmental
538 microorganisms as human pathogens. *American Society of Microbiology*.

539 Castella, V., M. Ruedi, L. Excoffier, C. Ibanez, R. Arlettaz *et al.*, 2000 Is the Gibraltar Strait a
540 barrier to gene flow for the bat *Myotis myotis* (Chiroptera: Vespertilionidae)? Mol.
541 Ecol. 9: 1761–1772.

542 Cockrum, E., 1969 Migration in the guano bat, *Tadarida brasiliensis*. Misc Publ Mus Nat Hist
543 Univ Kans. 51: 303–336.

544 Elshire, R. J., J. C. Glaubitz, Q. Sun, J. A. Poland, K. Kawamoto *et al.*, 2011 A robust, simple
545 genotyping-by-sequencing (GBS) approach for high diversity species (L. Orban, Ed.).
546 PLoS ONE 6: e19379.

547 Escobar, L. E., A. Lira-Noriega, G. Medina-Vogel, and A. T. Peterson, 2014 Potential for
548 spread of the white-nose fungus (*Pseudogymnoascus destructans*) in the Americas:
549 use of Maxent and NicheA to assure strict model transference. Geospatial Health
550 221–229.

551 Excoffier, L., I. Dupanloup, E. Huerta-Sánchez, V. C. Sousa, and M. Foll, 2013 Robust
552 Demographic Inference from Genomic and SNP Data. PLOS Genet. 9: e1003905.

553 Field, K. A., J. Johnson, T. Lilley, S. Reeder, E. Rogers *et al.*, 2015 The white-nose syndrome
554 transcriptome: activation of anti-fungal host responses in wing tissue of hibernating
555 bats. Plos Pathog. 11: e1005168.

556 Frick, W. F., J. F. Pollock, A. C. Hicks, K. E. Langwig, D. S. Reynolds *et al.*, 2010 An emerging
557 disease causes regional population collapse of a common North American bat
558 species. Science 329: 679–682.

559 Galaz, J., J. Yañez, A. Gantz, and D. Martínez, 2006 Orden Chiroptera. Pp. 67–89 in
560 Mamíferos de Chile (A. Muñoz-Pedreros and J.Yañez, eds.)., in *Mamíferos de Chile*,
561 Centro de Estudios Agrarios y Ambientales, Valdivia, Chile.

562 Gardner, A. (ed.), 2007 *Mammals of South America, Volume 1*. University of Chicago Press,
563 Chicago, Illinois.

564 Glass, B. P., 1982 Seasonal movements of Mexican freetail bats *Tadarida brasiliensis*
565 *mexicana* banded in the Great Plains. Southwest. Nat. 27: 127–133.

566 Hewitt, G. M., 1999 Post-glacial re-colonization of European biota. Biol. J. Linn. Soc. 68: 87–
567 112.

568 Hewitt, G. M., 1996 Some genetic consequences of ice ages, and their role in divergence and
569 speciation. Biol. J. Linn. Soc. 58: 247–276.

570 Holz, P., J. Hufschmid, W. Boardman, P. Cassey, S. Firestone *et al.*, 2019 Does the fungus
571 causing white-nose syndrome pose a significant risk to Australian bats? Wildl. Res.
572 46: 657–668.

573 Hoyt, J. R., K. E. Langwig, J. Okoniewski, W. F. Frick, W. B. Stone *et al.*, 2014 Long-term
574 persistence of *Pseudogymnoascus destructans*, the causative agent of white-nose
575 syndrome, in the absence of bats. EcoHealth.

576 Huntley, B., and T. Webb, 1989 Migration: species' response to climatic variations caused by
577 changes in the earth's orbit. J. Biogeogr. 5–19.

578 Jaarola, M., and H. Tegelström, 1995 Colonization history of north European field voles
579 (*Microtus agrestis*) revealed by mitochondrial DNA. Mol. Ecol. 4: 299–310.

580 Johnson, J. S., D. M. Reeder, T. M. Lilley, G. Á. Czirják, C. C. Voigt *et al.*, 2015 Antibodies to
581 *Pseudogymnoascus destructans* are not sufficient for protection against white-nose
582 syndrome. Ecol. Evol. 2203–2214.

583 Knopp, T., and J. Merilä, 2009 The postglacial recolonization of Northern Europe by *Rana*
584 *arvalis* as revealed by microsatellite and mitochondrial DNA analyses. Heredity 102:
585 174–181.

586 Koopman, K., 1967 The southernmost bats. J. Mammal. 48: 487–488.

587 Laine, V. N., T. M. Lilley, K. Norrdahl, and C. R. Primmer, 2013 Population genetics of
588 Daubenton's bat (*Myotis daubentonii*) in the Archipelago Sea, SW Finland. Ann. Zool.
589 Fenn. 50: 303–315.

590 Lemopoulos, A., S. Uusi-Heikkilä, A. Vasemägi, A. Huusko, H. Kokko *et al.*, 2017 Genome-
591 wide divergence patterns support fine-scaled genetic structuring associated with
592 migration tendency in brown trout. Can. J. Fish. Aquat. Sci. 75: 1680–1692.

Leopardi, S., D. Blake, and S. J. Puechmaille, 2015 White-nose syndrome fungus introduced from Europe to North America. Curr. Biol. 25: R217–R219.

Lilley, T., J. Anttila, and L. Ruokolainen, 2018 Landscape structure and ecology influence the spread of a bat fungal disease. Funct. Ecol. 32: 2483–2496.

Lilley, T. M., J. M. Prokkola, A. S. Blomberg, S. Paterson, J. S. Johnson *et al.*, 2019 Resistance is futile: RNA-sequencing reveals differing responses to bat fungal pathogen in Nearctic *Myotis lucifugus* and Palearctic *Myotis myotis*. Oecologia.

Lilley, T. M., J. M. Prokkola, J. S. Johnson, E. J. Rogers, S. Gronsky *et al.*, 2017 Immune responses in hibernating little brown myotis (*Myotis lucifugus*) with white-nose syndrome. Proc R Soc B 284: 20162232.

Lorch, J. M., C. U. Meteyer, M. J. Behr, J. G. Boyles, P. M. Cryan *et al.*, 2011 Experimental infection of bats with *Geomyces destructans* causes white-nose syndrome. Nature 480: 376-U129.

Lorch, J. M., L. K. Muller, R. E. Russell, M. O'Connor, D. L. Lindner *et al.*, 2013 Distribution and environmental persistence of the causative agent of white-nose syndrome, *Geomyces destructans*, in bat hibernacula of the Eastern United States. Appl. Environ. Microbiol. 79: 1293–1301.

Mann, G., 1978 Los pequeños mamiferos de Chile. Gayana Concepc. 40: 1–342.

Mansilla, C. A., R. D. McCulloch, and F. Morello, 2018 The vulnerability of the Nothofagus forest-steppe ecotone to climate change: Palaeoecological evidence from Tierra del Fuego (~53°S). Palaeogeogr. Palaeoclimatol. Palaeoecol. 508: 59–70.

614 McCracken, G. F., R. F. Bernard, M. Gamba-Rios, R. Wolfe, J. J. Krauel *et al.*, 2018 Rapid
615 range expansion of the Brazilian free-tailed bat in the southeastern United States,
616 2008–2016. J. Mammal. 99: 312–320.

617 Meierhofer, M. B., J. S. Johnson, S. J. Leivers, B. L. Pierce, J. E. Evans *et al.*, 2019 Winter
618 habitats of bats in Texas. PLOS ONE 14: e0220839.

619 Miller-Butterworth, C. M., M. J. Vonhof, J. Rosenstern, G. G. Turner, and A. L. Russell, 2014
620 Genetic structure of little brown bats (*Myotis lucifugus*) corresponds with spread of
621 white-nose syndrome among hibernacula. J. Hered. esu012.

622 Moritz, C., 1994 Defining 'Evolutionarily Significant Units' for conservation. Trends Ecol.
623 Evol. 9: 373–375.

624 Muller, L. K., J. M. Lorch, D. L. Lindner, M. O'Connor, A. Gargas *et al.*, 2013 Bat white-nose
625 syndrome: a real-time TaqMan polymerase chain reaction test targeting the
626 intergenic spacer region of *Geomyces destructans*. Mycologia 105: 253–259.

627 Nesbø, C. L., T. Fossheim, L. A. Vøllestad, and K. S. Jakobsen, 1999 Genetic divergence and
628 phylogeographic relationships among European perch (*Perca fluviatilis*) populations
629 reflect glacial refugia and postglacial colonization. Mol. Ecol. 8: 1387–1404.

630 Ommundsen, P., C. Lausen, and L. Matthias, 2017 First acoustic records of the Brazilian free-
631 tailed bat (*Tadarida brasiliensis*) in British Columbia. Northwest. Nat. 98: 132–136.

632 Orsini, L., J. Vanoverbeke, I. Swillen, J. Mergeay, and L. De Meester, 2013 Drivers of
633 population genetic differentiation in the wild: isolation by dispersal limitation,
634 isolation by adaptation and isolation by colonization. Mol. Ecol. 22: 5983–5999.

Ossa, G., 2016 Primer registro de la especie *Myotis chiloensis*, (Waterhouse, 1838) (Chiroptera, Vespertilionidae) en el Parque Nacional Alberto de Agostini (Región de Magallanes y Antártica Chilena). An. Inst. Patagon. 44: 85–88.

Ossa, G., J. S. Johnson, A. I. E. Puisto, V. Rinne, I. E. Sääksjärvi *et al.*, 2019 The Klingon batbugs: Morphological adaptations in the primitive bat bugs, *Bucimex chilensis* and *Primicimex cavernis*, including updated phylogeny of Cimicidae. Ecol. Evol. 9: 1736–1749.

Ossa, G., T. M. Lilley, A. G. Waag, M. Meierhofer, and J. Johnson, Submitted for publication Roosting ecology of the southernmost tree-dwelling bats, *Myotis chiloensis* and *Histiotus magellanicus*, in southern Tierra del Fuego.

Ossa, G., and Rodriguez-San Pedro, 2015 *Myotis chiloensis* (Chiroptera: Vespertilionidae). Mammal Species 47: 51–56.

Ponce, J. F., J. Rabassa, A. Coronato, and A. M. Borromei, 2011 Palaeogeographical evolution of the Atlantic coast of Pampa and Patagonia from the last glacial maximum to the Middle Holocene. Biol. J. Linn. Soc. 103: 363–379.

Rabassa, J., A. Coronato, and O. Martínez, 2011 Late Cenozoic glaciations in Patagonia and Tierra del Fuego: an updated review. Biol. J. Linn. Soc. 103: 316–335.

Raudabaugh, D. B., and A. N. Miller, 2013 Nutritional capability of and substrate suitability for *Pseudogymnoascus destructans*, the causal agent of wat white-nose syndrome. PLoS ONE 8: e78300.

655 Ruedi, M., B. Stadelmann, Y. Gager, E. J. P. Douzery, C. M. Francis *et al.*, 2013 Molecular
656 phylogenetic reconstructions identify East Asia as the cradle for the evolution of the
657 cosmopolitan genus Myotis (Mammalia, Chiroptera). Mol. Phylogenet. Evol. 69: 437–
658 449.

659 Scholthof, K.-B. G., 2007 The disease triangle: pathogens, the environment and society. Nat.
660 Rev. Microbiol. 5: 152–156.

661 Semenza, J. C., and B. Menne, 2009 Climate change and infectious diseases in Europe.
662 Lancet Infect. Dis. 9: 365–375.

663 Serre, J., 2006 *Génétique des populations*. Dunod, Paris.

664 Sérsic, A. N., A. Cosacov, A. A. Cocucci, L. A. Johnson, R. Pozner *et al.*, 2011 Emerging
665 phylogeographical patterns of plants and terrestrial vertebrates from Patagonia.
666 Biol. J. Linn. Soc. 103: 475–494.

667 Tegelström, H., 1987 Transfer of mitochondrial DNA from the northern red-backed vole
668 (*Clethrionomys rutilus*) to the bank vole (*C. glareolus*). J. Mol. Evol. 24: 218–227.

669 Turbill, C., and J. A. Welbergen, 2019 Anticipating white-nose syndrome in the Southern
670 Hemisphere: Widespread conditions favourable to *Pseudogymnoascus destructans*
671 pose a serious risk to Australia's bat fauna. Austral Ecol. 45: 89–96.

672 Turner, G. G., D. M. Reeder, and J. T. H. Coleman, 2011 A five-year assessment of mortality
673 and geographic spread of white-nose syndrome in North American bats and a look to
674 the future. Bat Res. News 52: 13–27.

675 Verant, M. L., J. G. Boyles, W. Waldrep, G. Wibbelt, and D. S. Blehert, 2012 Temperature-
676 dependent growth of *Geomyces destructans*, the fungus that causes bat white-nose
677 syndrome. Plos One 7: e46280.

678 Vonhof, M. J., A. L. Russell, and C. M. Miller-Butterworth, 2015 Range-wide genetic analysis
679 of little brown bat (*Myotis lucifugus*) populations: estimating the risk of spread of
680 White-nose syndrome. PLoS ONE 10: e0128713.

681 Warnecke, L., J. M. Turner, T. K. Bollinger, J. M. Lorch, V. Misra *et al.*, 2012 Inoculation of
682 bats with European *Geomyces destructans* supports the novel pathogen hypothesis
683 for the origin of white-nose syndrome. Proc. Natl. Acad. Sci. U. S. A. 109: 6999–7003.

684 Wilder, A. P., T. H. Kunz, and M. D. Sorenson, 2015 Population genetic structure of a
685 common host predicts the spread of white-nose syndrome, an emerging infectious
686 disease in bats. Mol. Ecol. 24: 5495–5506.

687 Zukal, J., H. Bandouchova, T. Bartonicka, H. Berkova, V. Brack *et al.*, 2014 White-nose
688 syndrome fungus: a generalist pathogen of hibernating bats. Plos One 9: e97224.

689 Zukal, J., H. Bandouchova, J. Brichta, A. Cmokova, K. S. Jaron *et al.*, 2016 White-nose
690 syndrome without borders: *Pseudogymnoascus destructans* infection tolerated in
691 Europe and Palearctic Asia but not in North America. Sci. Rep. 6: 19829.

692

693 Figure captions:

694 Figure 1. Sampling locations and groupings for genetic sampling of *Myotis chiloensis* in Chile
695 (A). The two most important principal components calculated from allele frequencies
696 explain 15.8% of the total nucleotide variation (B).

697 Figure 2. Biogeographical ancestry (admixture) analysis based on nucleotide polymorphisms.
698 Each vertical bar represents an individual, ordered by latitude. Red, green, blue and purple
699 colours indicate the relative genetic contributions of ancestral populations inhabiting
700 regions 1-4, respectively.

701 Fig. 3. The correlation between geographic and genetic distances between individuals.
702 Geographic distances are measured in kilometres, and genetic distances as Euclidean
703 principal component distances from the reference individual (sample 700). Dashed lines
704 represent 95% confidence interval for the linear model. The violin plot highlights the
705 differences between model residuals for each study region. Residual distributions that differ
706 significantly from zero after Bonferroni correction for multiple testing are marked with * (P
707 < 0.05) and *** ($P < 0.0001$).

708

Numeric region	Number of individuals (A)	Number of duplicates (B)	male / female	Mean observed heterozygosity (95% confidence interval)	Mean expected heterozygosity (95% confidence interval)	Inbreeding coefficient *F*	Unique SNPs
1	20	6	16/4	0.2550 (0.2530-0.2570)	0.2793 (0.2777-0.2809)	0.0868 (0.0813 - 0.0925)	8.6%
2	19	6	9/10	0.2536 (0.2514-0.2557)	0.2765 (0.2749-0.2780)	0.08286 (0.0773- 0.0891)	4.4%
3	14	9	7/7	0.2872 (0.2848-0.2896)	0.2993 (0.29762-0.3009)	0.0404 (0.0343 – 0.0463)	3.6%
4	13	9	5/8	0.3248 (0.3221-0.3275)	0.3335 (0.3316-0.3352)	0.0261 (0.0197 – 0.0326)	2.5%
tot.	**66**	**30**					

Table 1. Individuals and samples per region.

	F_{ST} and mean geographic distance (*km*)			
	Region 4	Region 3	Region 2	Region 1
Region 4		*970.9*	*1550.3*	*2266.9*
Region 3	0.075***		*588.7*	*1326.6*
Region 2	0.089***	0.041***		*757.0*
Region 1	0.113***	0.072***	0.040***	

Table 2. Nei's pairwise F_{ST} and geographic distances (in italics) between populations inhabiting the four geographic regions. The significance level (P<0.01) of the F_{ST} statistics is denoted with ***.

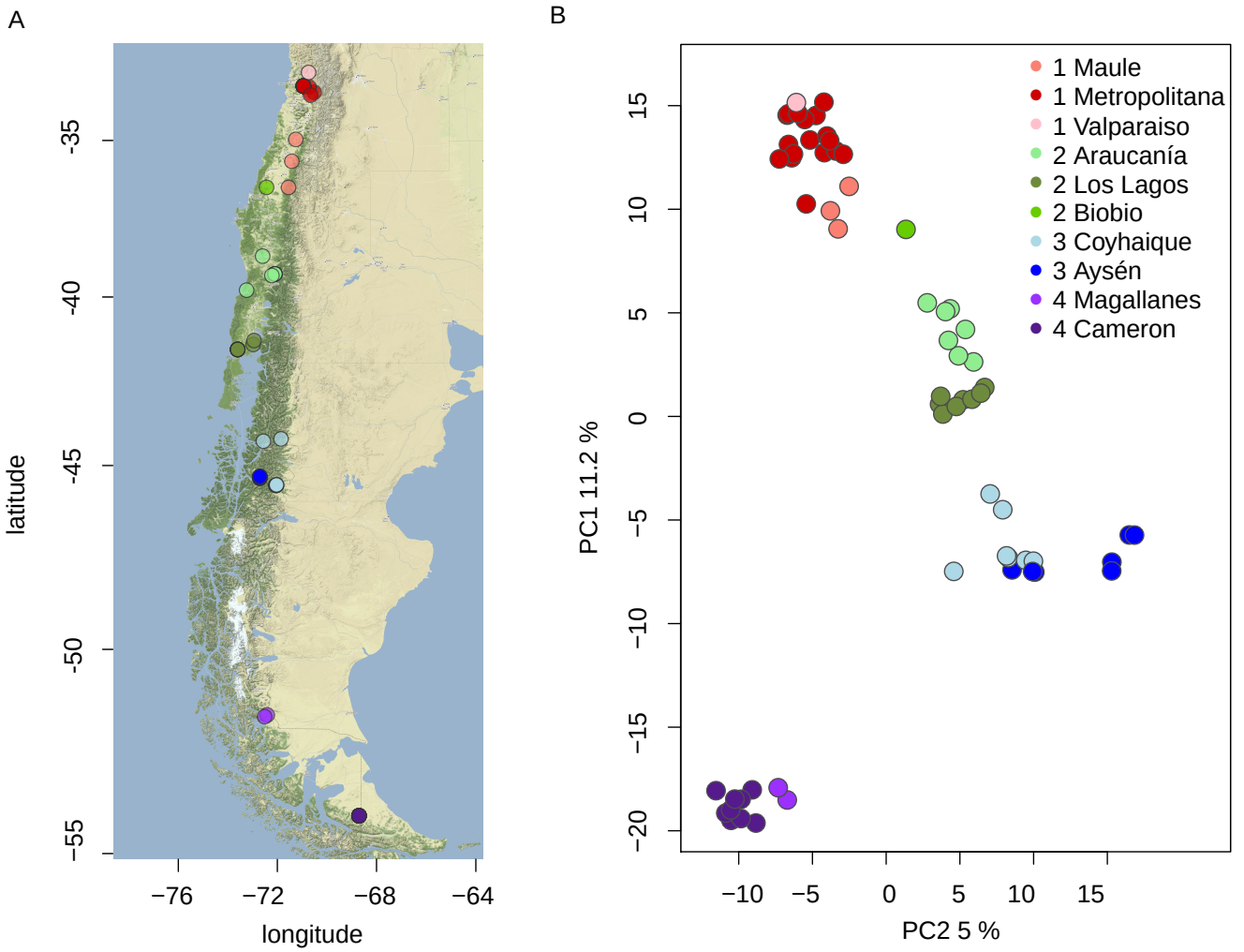
A
B
latitude
longitude
-35
-40
-45
-50
−55
−76
−72
−68
−64
PC1 11.2 %
PC2 5 %
15
10
5
0
−5
−10
−15
−20
−10
−5
0
5
10
15
1 Maule
1 Metropolitana
1 Valparaiso
2 Araucanía
2 Los Lagos
2 Biobio
3 Coyhaique
3 Aysén
4 Magallanes
4 Cameron

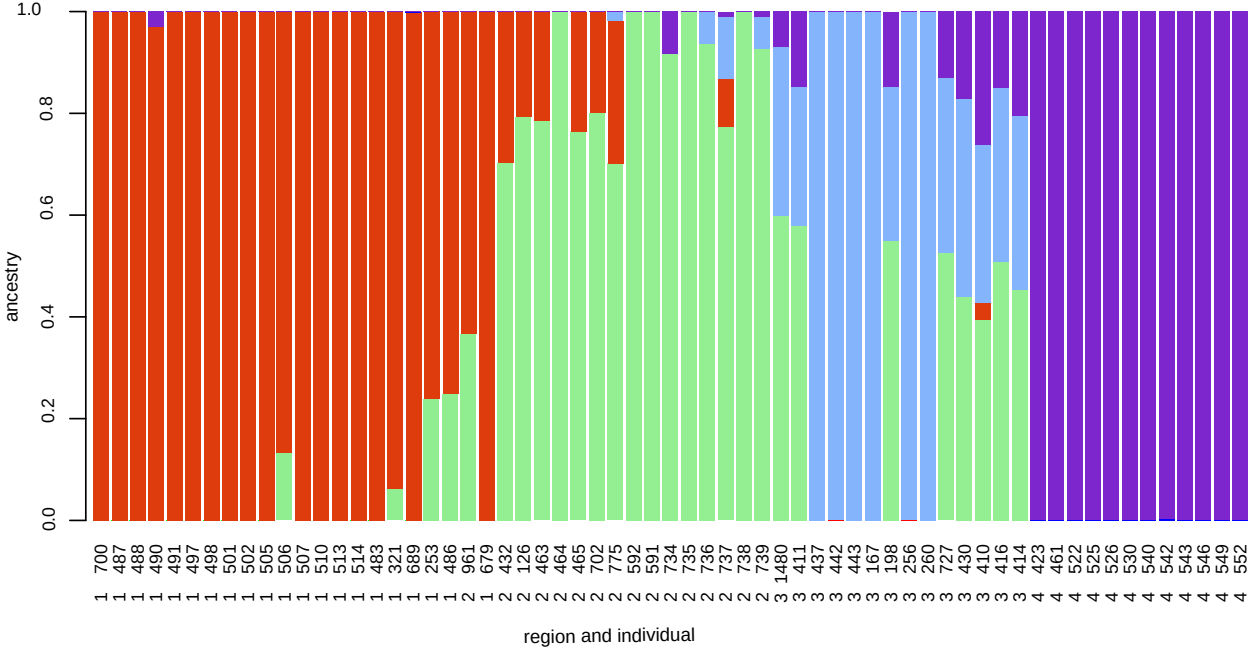
ancestry
0.0
0.2
0.4
0.6
0.8
1.0
1 700
1 487
1 488
1 490
1 491
1 497
1 498
1 501
1 502
1 505
1 506
1 507
1 510
1 513
1 514
1 483
1 321
1 689
1 253
1 486
2 961
1 679
2 432
2 126
2 463
2 464
2 465
2 702
2 775
2 592
2 591
2 734
2 735
2 736
2 737
2 738
2 739
3 1480
3 411
3 437
3 442
3 443
3 167
3 198
3 256
3 260
3 727
3 430
3 410
3 416
3 414
4 423
4 461
4 522
4 525
4 526
4 530
4 540
4 542
4 543
4 546
4 549
4 552
region and individual

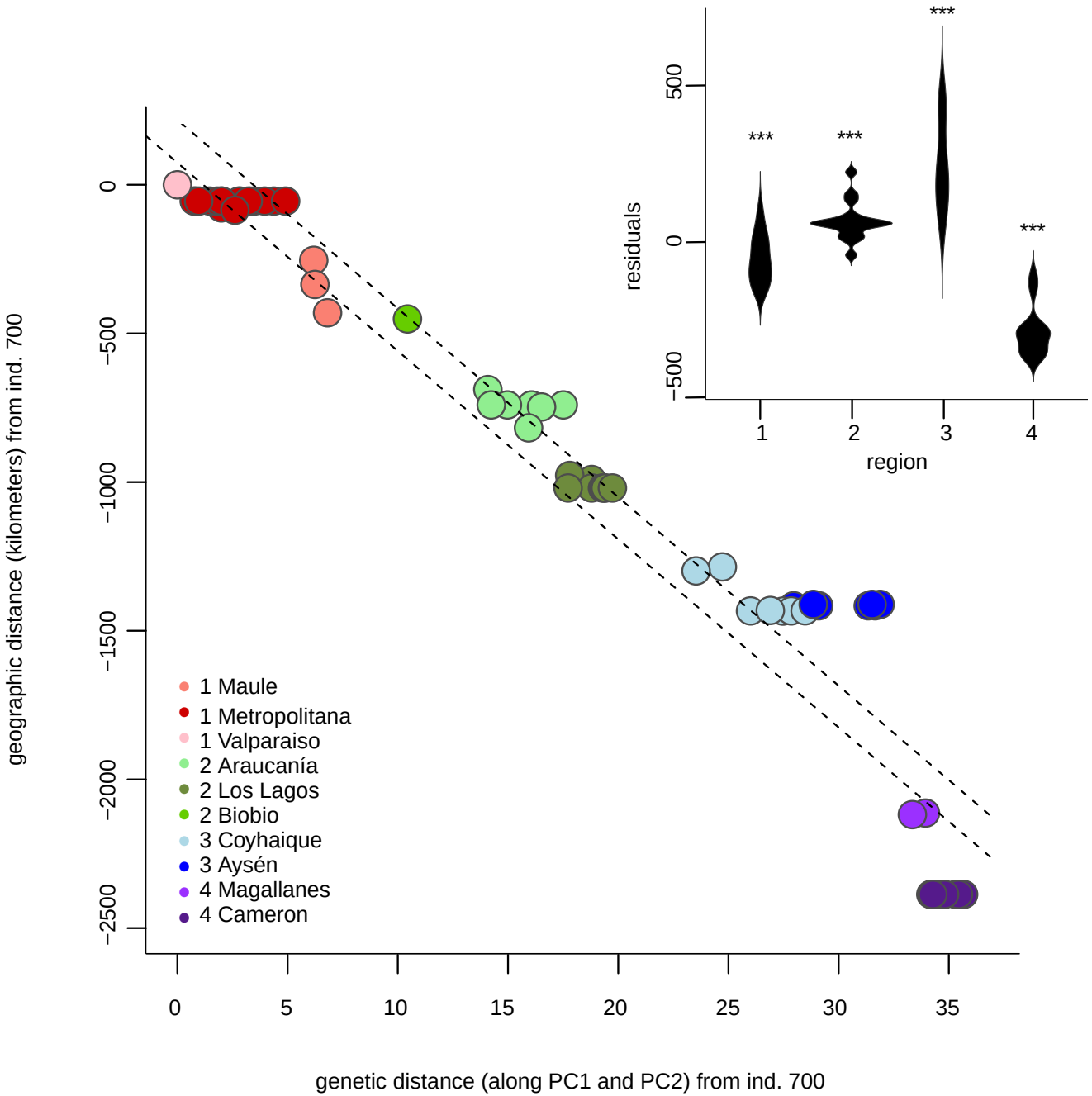
geographic distance (kilometers) from ind. 700
genetic distance (along PC1 and PC2) from ind. 700
0
−500
−1000
−1500
−2000
−2500
0
5
10
15
20
25
30
35
1 Maule
1 Metropolitana
1 Valparaiso
2 Araucanía
2 Los Lagos
2 Biobio
3 Coyhaique
3 Aysén
4 Magallanes
4 Cameron
residuals
500
0
−500
***
***
***
***
1
2
3
4
region